



Environmental magnesium ion affects global gene expression, motility, biofilm formation and virulence of *Vibrio parahaemolyticus*

Xue Li^{a,1}, Xiaobai Zhang^{b,1}, Miaomiao Zhang^a, Xi Luo^a, Tingting Zhang^a, Xianjin Liu^{c,**}, Renfei Lu^{a,***}, Yiquan Zhang^{a,*}

^a Department of Clinical Laboratory, Affiliated Nantong Hospital 3 of Nantong University, Nantong Third People's Hospital, Nantong, 226006, Jiangsu, China

^b Department of Respiratory Medicine, Affiliated Nantong Hospital 3 of Nantong University, Nantong Third People's Hospital, Nantong, 226006, Jiangsu, China

^c Department of Infection, Affiliated Nantong Hospital 3 of Nantong University, Nantong Third People's Hospital, Nantong, 226006, Jiangsu, China

ARTICLE INFO

Keywords:

Vibrio parahaemolyticus

Mg²⁺

Motility

Biofilm

Virulence

Gene expression

ABSTRACT

Vibrio parahaemolyticus is widely distributed in marine ecosystems. Magnesium ion (Mg²⁺) is the second most abundant metal cation in seawater, and plays important roles in the growth and gene expression of *V. parahaemolyticus*, but lacks the detailed mechanisms. In this study, the RNA sequencing data demonstrated that a total of 1494 genes was significantly regulated by Mg²⁺. The majority of the genes associated with lateral flagella, exopolysaccharide, type III secretion system 2, type VI secretion system (T6SS) 1, T6SS2, and thermostable direct hemolysin were downregulated. A total of 18 genes that may be involved in c-di-GMP metabolism and more than 80 genes encoding putative regulators were also significantly and differentially expressed in response to Mg²⁺, indicating that the adaptation process to Mg²⁺ stress may be strictly regulated by complex regulatory networks. In addition, Mg²⁺ promoted the proliferative speed, swimming motility and cell adhesion of *V. parahaemolyticus*, but inhibited the swarming motility, biofilm formation, and c-di-GMP production. However, Mg²⁺ had no effect on the production of capsular polysaccharide and cytotoxicity against HeLa cells. Therefore, Mg²⁺ had a comprehensive impact on the physiology and gene expression of *V. parahaemolyticus*.

1. Introduction

Vibrio parahaemolyticus, a seafood borne pathogen, commonly causes acute gastroenteritis in human [1]. Pathogenicity of *V. parahaemolyticus* is correlated with thermostable direct hemolysin (TDH) and/or TDH-related hemolysin (TRH), both of which possess hemolytic activity, but only TDH induces β-type hemolysis on Wagatsuma agar, termed as Kanagawa phenomenon (KP) [2]. However, TDH and TRH are not the only virulence factors of *V. parahaemolyticus*. Other factors such as type III secretion system (T3SS), type VI secretion system (T6SS), capsular polysaccharide (CPS) and extracellular proteases are also involved in the pathogenesis of *V. parahaemolyticus* [3,4]. Pathogenic *V. parahaemolyticus* isolates harbor two sets of genes for T3SS on chromosomes, termed as T3SS1 and T3SS2, respectively [5]. T3SS1 has cytotoxicity and lethal activity, while T3SS2 mainly possesses enterotoxigenicity [6]. *V. parahaemolyticus* also possesses two kinds of T6SS gene

clusters, T6SS1 and T6SS2, respectively [7]. T6SS1 has anti-bacterial activity, whereas T6SS2 can help bacteria adhere to host cells [7,8].

V. parahaemolyticus is capable of accumulating on the surface and seafood to form biofilms, which are extracellular polymeric substance matrix-enclosed bacterial communities that endow bacteria with high resistance to adverse conditions [9]. Biofilm formation by *V. parahaemolyticus* depends upon some specific structures including flagella, type IV pili and exopolysaccharide (EPS) and is strictly regulated by regulatory networks consist of regulators, quorum sensing (QS) and cycle di-GMP (c-di-GMP) signaling [10]. Flagella promote bacteria to move toward and along the surface, and thus are required for the initial stages of biofilm formation [10]. *V. parahaemolyticus* has a single polar flagellum for swimming in liquid and multiple lateral flagella for swarming over surfaces [11]. Loss of polar flagellum prevents *V. parahaemolyticus* to form mature biofilms [12]. Type VI pili promote the interactions between bacterial cells and the surface, and thus are

* Corresponding author.

** Corresponding author.

*** Corresponding author.

E-mail addresses: lxj009650@sina.com (X. Liu), rainman78@163.com (R. Lu), zhangyiquanq@163.com (Y. Zhang).

¹ These authors contributed equally to this work.

required for biofilm formation [10]. Two kinds of type IV pili, termed as mannose-sensitive haemagglutinin (MSHA) and chitin-regulated pili (ChiRP), are produced by *V. parahaemolyticus* [13]. MSHA is beneficial for bacteria to adhere to the surface, while ChiRP can promote bacterial agglutination [14]. EPS is a major fraction of the biofilm matrix [15]. In *V. parahaemolyticus*, the *cpsA-K* and *scvA-O* gene clusters are involved in the biosynthesis of EPS [16]. Loss of *cps* or *scv* genes decreased the amount of biofilms formed by *V. parahaemolyticus* [16].

The second messenger c-di-GMP is widely used by bacteria to control bacterial behaviors including motility, biofilm formation, and virulence [17]. Elevated c-di-GMP level enhances biofilm formation, but decreases bacterial motility and virulence factor production [17]. c-di-GMP is made from GTP by the GGDEF domain of diguanylate cyclase (DGC) and degraded by the EAL or HD-GYP domain of phosphodiesterase (PDE) [17]. Previously, a total of 62 genes were predicted to be involved in the metabolism of c-di-GMP in *V. parahaemolyticus* [18]. Of these, *scrC* and *scrG* encode GGDEF-EAL-domain containing proteins, which function as PDEs to degrade c-di-GMP [19,20]. In addition, *scrO*, *gefA*, *scrJ* and *scrL* encode GGDEF-domain containing proteins, while *lafV*, *tpdA* and *vopY* encode EAL-domain containing proteins, and these genes are all involved in controlling motility and/or biofilm formation [21–25].

V. parahaemolyticus is a Gram-negative halophilic bacterium that widely distributed in marine ecosystems and can thrive in sodium chloride concentrations between 0.5 and 10%. The average content of Na⁺ in seawater is about 450 mM, making it the most abundant metal cation [26]. The second most abundant metal cation is magnesium ion (Mg²⁺), which can reach an average of approximately 53 mM [26]. Mg²⁺ has a wide range of impact on marine microorganisms. For example, Mg²⁺ supports the growth of *V. alginolyticus* at concentrations between 0.3 and 2.1%, and the swarming motility at temperatures between 20 and 28 °C [27]. In addition, Mg²⁺ promotes migration of *V. fischeri* by enhancing flagellation and decreasing c-di-GMP production [28–30]. Moreover, Mg²⁺ has a marked beneficial effect on the recovery of heat-injured *V. parahaemolyticus* that increases uptake of Mg²⁺ for stability and repair [31,32]. Mg²⁺ promotes the secretion of proteins including T3SS1 effectors in *V. parahaemolyticus* [33,34]. Mg²⁺ only can also promote the expression level of GbpA, an important colonization factor of *V. parahaemolyticus* [35]. Therefore, Mg²⁺ plays an important role in the growth and gene expression of *V. parahaemolyticus*. However, the detailed roles of Mg²⁺ in gene expression and bacterial behaviors are still unknown in *V. parahaemolyticus*. In this work, we aimed to analyze the effects of Mg²⁺ on the motility, biofilm formation, virulence, and gene expression of *V. parahaemolyticus*.

2. Materials and methods

2.1. Bacterial strain and growth conditions

V. parahaemolyticus RIMD2210633 was used throughout the work [13]. Unless stated otherwise, *V. parahaemolyticus* was grown in 2.5% (w/v) Bacto heart infusion (HI) broth (BD Biosciences, USA) at 37 °C with aeration. An overnight cell culture was diluted 50-fold into 5 ml HI broth and then cultured at 37 °C to OD₆₀₀ = 1.4 (defined here as bacterial seed). The bacterial seed was diluted 1000-fold into 5 ml HI broth supplemented with various concentrations of MgCl₂ (0, 3.5, 35 and 55 mM) for the further growth.

2.2. Assessment of the impact of Mg²⁺ on growth

The bacterial seed was diluted 1000-fold into 10 ml HI broth containing 0, 3.5, 35 or 55 mM MgCl₂ in a bacteria-free plastic centrifuge tube, mixed thoroughly, and then divided into a 96 well cell culture plate. Each well contained 200 µl of bacterial suspension. Twelve biological replicates were set for each concentration. Growth curves were created using a microbial growth curve analyzer MGC-200 (Ningbo Scientz Biotechnology Co. Ltd., China) by monitoring the OD₆₀₀ values

of each culture at 20 min intervals. Target temperature and oscillation frequency were 37 °C and 800, respectively.

2.3. RNA extraction and RNA sequencing (RNA-seq)

The bacterial seed was diluted 1:1000 into 5 ml HI broth or HI broth supplemented with 55 mM MgCl₂, and then incubated at 37 °C with aeration to an OD₆₀₀ value of 1.5. Bacterial cells were harvested for the preparation of total RNA using TRIzol Reagent (Invitrogen, USA). RNA concentration was determined by a Nanodrop 2000. RNA integrity was evaluated by agarose gel electrophoresis. The rRNA removal and mRNA enrichment were performed using an Illumina/Ribo-Zero™ rRNA Removal Kit (bacteria) (Illumina, USA). RNA-related manipulations including total RNA concentration were performed in Sangon Biotech (Shanghai, China).

cDNA sequencing was performed on an Illumina HiSeq platform [36]. Raw reads filtration and clean reads alignment were performed as previously described [37]. Gene expression in bacterial cells grown in HI broth supplemented with 55 mM MgCl₂ (test group) were compared with that in bacterial cells grown in HI broth (reference group). DESeq (v1.12.4) was applied to identify the significantly differentially expressed genes (DEGs) [38], which were filtered as those with pValue ≤ 0.01 and absolute FoldChange ≥ 2. DEGs were also analyzed by the Gene Ontology (GO) enrichment, the Kyoto Encyclopedia of Genes and Genomes (KEGG) pathway enrichment and the Cluster of Orthologous Groups of proteins (COG) database [39–41].

2.4. Quantitative real-time PCR (qPCR)

V. parahaemolyticus RIMD2210633 was grown in HI broth or HI broth supplemented with 55 mM MgCl₂ at 37 °C with aeration to an OD₆₀₀ value of 1.5. Bacterial cells were harvested for the extraction of total RNA. cDNA was generated from 0.8 µg of total RNA using a FastKing First Strand cDNA Synthesis Kit (Tiangen Biotech, China). The qPCR assay was performed using a LightCycler 480 (Roche, Switzerland) together with SYBR Green master mix (Tiangen Biotech, China). Relative mRNA level of each target gene was detected by using the classic 2^{-ΔΔCt} method with 16S rRNA gene as the internal control [42]. Primers used in this study are listed in Table S1.

2.5. Crystal violet (CV) staining assay

CV staining assay was performed similarly as previously described [43–47]. Briefly, the bacterial seed was diluted 50-fold into 2 ml HI broth or HI broth supplemented with 55 mM Mg²⁺ in a 24-well cell culture plate, and then incubated at 30 °C with shaking at 150 rpm for 12 h. Planktonic cells were collected for detection of OD₆₀₀ values. Attached biofilms were washed with deionized water, and then stained with 0.1% CV. Bound CV was dissolved with 2.5 ml of 20% acetic acid, followed by determination of OD₅₇₀ values. Relative biofilm was expressed as OD₅₇₀/OD₆₀₀.

2.6. Colony morphology assay

Colony morphology assay was performed similarly as previously described [44]. Briefly, 2 µl of bacterial seed was taken to spot on an HI plate or HI plate supplemented with 55 mM Mg²⁺, and then statically incubated at 37 °C for 24 h.

2.7. Quantification of intracellular c-di-GMP level

Intracellular c-di-GMP level was similarly quantified as previously described [44,48]. Briefly, the bacterial seed was diluted 1000-fold into 5 ml HI broth supplemented with 0 and 55 mM MgCl₂, respectively, and then incubated at 37 °C with aeration to an OD₆₀₀ value of 1.5. Bacterial cells were harvested from 1 ml bacterial culture and then resuspended in

2 ml ice-cold phosphate buffered saline (PBS). The bacterial suspension was incubated at 100 °C for 5 min, sonicated for 15 min (power 100%, frequency 37 kHz) in the ice-water bath condition, and then centrifuged at 12000 rpm and 4 °C for 5 min. Total proteins and c-di-GMP levels in the supernatant were determined using a Pierce BCA Protein Assay kit (ThermoFisher Scientific, USA) and c-di-GMP Enzyme-linked Immunosorbent Assay (ELISA) Kit (Mskbio, China), respectively. The intracellular c-di-GMP concentration was expressed as pmol/g protein.

2.8. Motility assays

The swimming and swarming motility assays were similarly performed as previously described [49,50]. Briefly, 2 µl of the bacterial seed were inoculated into a semi-solid HI plate containing 0.5% (w/v) Difco Noble agar (BD Biosciences, USA) for swimming motility or spotted on a HI plate containing 2.0% (w/v) Difco noble agar for swarming motility. The HI plate was supplemented with 0 or 55 mM MgCl₂. The diameters of swimming and swarming areas were measured after incubation at 37 °C.

2.9. Detection of CPS phase variation

CPS phase variation was similarly detected as previously described [44]. Briefly, a small portion of bacterial seeds was streaked onto a HI plate or HI plate supplemented with 55 mM MgCl₂, followed by incubated at 37 °C for 24 h.

2.10. Cytotoxicity against HeLa cells

Cytotoxicity against HeLa cells was performed similarly as previously described [51]. Briefly, the bacterial seed was diluted 1000-fold into 5 ml HI broth supplemented with 0 and 55 mM MgCl₂, respectively, and then incubated at 37 °C with aeration to an OD₆₀₀ value of 1.5. Bacterial cells were harvested by centrifuge, washed three times with PBS, and then serially diluted with the pre-warmed Dulbecco's modified Eagle's medium (DMEM) lacking phenol red for colony forming unit (CFU) detection and infection. HeLa cells were infected with 10⁶ CFU of *V. parahaemolyticus* for 3 h at a multiplicity of infection (MOI) of 2.5. The release of lactate dehydrogenase (LDH) was measured by using a CytoTox 96® Non-Radioactive Cytotoxicity Assay kit (Promega, USA).

2.11. Adhesion to HeLa cells

Adhesion assay was performed similarly as previously described [44]. Briefly, HeLa cell monolayers were maintained in DMEM supplemented with 10% fetal bovine serum (FBS, Invitrogen) at 37 °C with 5% CO₂. The bacterial seed was diluted 1000-fold into 5 ml HI broth supplemented with 0 and 55 mM MgCl₂, respectively, and incubated at 37 °C with aeration to an OD₆₀₀ value of 1.5. Bacterial cells were collected, washed, re-suspended in DMEM, and then used to infect the cell monolayers at a MOI of 10. Bacterial cells were also added to empty wells to determine the input CFU of *V. parahaemolyticus*. After incubation for 90 min, the cell monolayers were washed three times with PBS and lysed with 1% Triton X-100. The lysates and input bacteria were serially diluted 10-fold and counted on LB plates. Percent adherence was calculated as adhered CFU/input CFU.

2.12. KP test

KP test was performed similarly as previously described [52]. Briefly, 5 µl of bacterial seed were inoculated onto Wagatsuma agar (CHROMagar, China) containing 5% rabbit red blood cells (RBCs) or 5% RBCs together with 55 mM MgCl₂. The diameters of the β-hemolysin zone were measured after incubation at 25 °C for 24 h.

2.13. Experimental replicates and statistical methods

Each experiment except for RNA-seq was performed at least two independent times with at least three biological replicates in each time. The numerical results were expressed as the mean ± standard deviation (SD). Paired Student's *t*-tests or two-way ANOVA with Tukey's post hoc corrections for multiple comparisons was applied to calculate statistical significance, with a *P* value less than 0.05 considered significant.

3. Results and discussion

3.1. Mg²⁺ enhanced the proliferative speed of *V. parahaemolyticus*

V. parahaemolyticus can survive in 300 mM Mg²⁺, a condition which is toxic to many other microorganisms [33]. However, the effects of low levels of Mg²⁺ on the growth of *V. parahaemolyticus* have not been investigated previously. In this work, the growth curves of *V. parahaemolyticus* in HI broth supplemented with 0, 3.5, 35 and 55 mM MgCl₂ were measured, respectively, to assess whether Mg²⁺ has some effects on the bacterial growth. As shown in Fig. 1, the addition of Mg²⁺ significantly increased the proliferative speed of *V. parahaemolyticus* in HI broth (*P* < 0.05). The higher the molar concentration of Mg²⁺ was, the faster the proliferative speed was. In addition, Mg²⁺ was also able to shorten the growth adaptation period of *V. parahaemolyticus*. However, it must be noticed that the data for the growth analysis was based on the measurement of OD₆₀₀ values, which may not accurately reflect the alive cell count. A previous study showed that Mg²⁺ was able to maintain the stability and repair of membrane and/or ribosome of *V. parahaemolyticus* [32]. Therefore, we might conclude that Mg²⁺ could promote the proliferative speed of *V. parahaemolyticus*. Due to the average Mg²⁺ content in seawater being about 53 mM [26], bacteria were cultured under growth conditions of 0 and 55 mM Mg²⁺, and harvested at mid-log phase (OD₆₀₀ equals to approximately 1.5 when grown in a test tube) for the following experiments.

3.2. Mg²⁺ affected global gene expression of *V. parahaemolyticus*

The gene expression profile of *V. parahaemolyticus* grown in HI broth supplemented with 55 mM Mg²⁺ (test) was compared with that grown in HI broth (reference) by RNA-seq to investigate the expression of genes affected by Mg²⁺. The raw data of RNA-seq were deposited in the online

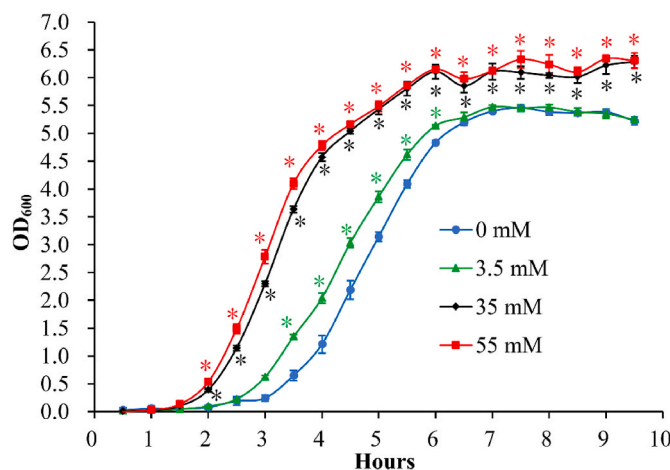


Fig. 1. Growth curves of *V. parahaemolyticus*. *V. parahaemolyticus* RIMD2210633 was cultured with HI broth supplemented with different molar concentrations of MgCl₂ in a 96 well cell culture plate, and then grown at 37 °C with shaking at 800 rpm in a microbial growth curve analyzer MGC-200. The growth curves were created by monitoring the OD₆₀₀ values of each culture at 20 min intervals. Experiments were performed at least two times with twelve replicates per trial for each condition. *, *P* < 0.05.

database Sequence Read Archive (accession number: PRJNA1035152). There are 1494 genes in total that were significantly and differentially expressed in response to Mg^{2+} (Fig. 2a), accounting for more than 30.9% of total genes of *V. parahaemolyticus* RIMD 2210633 [13]. Of these, 868 genes were up-regulated and 626 genes were down-regulated (Fig. 2a). The KEGG enrichment results showed that 23 DEGs were involved in organismal systems, 454 DEGs in metabolism, 70 DEGs in genetic information processing, 160 DEGs in environmental information processing, and 89 DEGs in cellular processes (Fig. 2b). The GO term results showed that a total of 395 DEGs were enriched in biological process (206 DEGs), molecular function (84 DEGs) and cellular component (105 DEGs) (Fig. 2c). The results of COG enrichment showed that DEGs were divided into 20 functional categories, mainly including function unknown, general function prediction only, amino acid transport and metabolism, transcription, and signal transduction mechanisms (Fig. 2d). The detailed information about DEGs is listed in Table S2.

3.3. Validation of RNA-seq results by qPCR

qPCR was employed to validate the results of RNA-seq. A total of 26 genes were selected as the target genes (Table 1). As shown in Fig. 3, the expression trends of all the target genes confirmed by qPCR were

consistent with those clarified by RNA-seq, suggesting that the RNA-seq results were reliable.

3.4. DEGs involved in motility

There are approximately 50 polar and 40 lateral flagellar genes in *V. parahaemolyticus* chromosomes 1 and 2, respectively [11]. The transcriptomic data in this work showed that transcription of 19 polar flagellar genes was differentially regulated by the additional Mg^{2+} , including 13 upregulated and 6 downregulated genes (Table 1). In addition, 20 lateral flagellar genes were also significantly and differentially expressed in response to Mg^{2+} , but only two of them (VPA1540 and VPA1546) were upregulated, while the others were downregulated (Table 1). The swimming and swarming motility were further investigated to detect whether Mg^{2+} -dependent differential expression of flagellar genes affect the motor capacities of *V. parahaemolyticus*. As shown in Fig. 4, addition of Mg^{2+} significantly increased the swimming motility but decreased the swarming motility of *V. parahaemolyticus* compared with the conditions without additional Mg^{2+} at all time points tested except for the first hour's growth ($P < 0.05$). Although expressing trends of flagellar genes not fully matched with motility-related phenotypes, the data presented here indicated that Mg^{2+} promoted

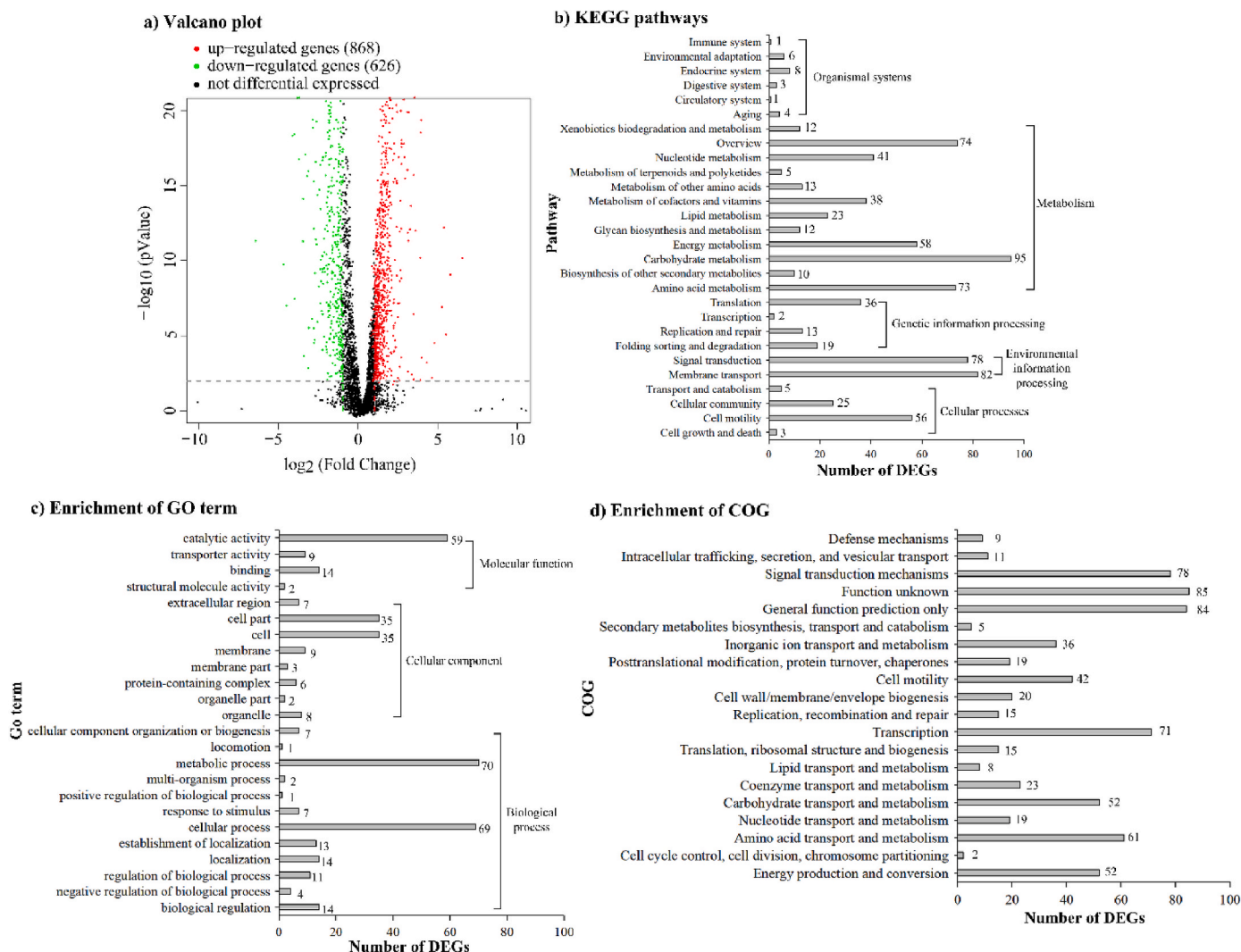


Fig. 2. Mg^{2+} affected global gene expression of *V. parahaemolyticus* RIMD2210633. a) Volcano plot. Red, green and black points represent the up-regulated, down-regulated and no-differential expressed genes, respectively. b) Kyoto Encyclopedia of Genes and Genomes (KEGG) enrichment for the pathways of DEGs involved. c) Enrichment of gene ontology (GO) term. d) Cluster of Orthologous Groups of proteins (COG). The number on the top of each bar in b, c and d indicates the number of enriched DEGs. (For interpretation of the references to colour in this figure legend, the reader is referred to the Web version of this article.)

Table 1
Selected DEGs.

Gene ID	Name	Fold change	pValue	Products
c-di-GMP				
VP0376		2.1344	0.004801546	EAL domain-containing protein
VP1289		2.1861	2.09E-05	GGDEF domain-containing protein
VP1423		2.1534	4.81E-09	HD-GYP domain-containing protein
VP1768		2.4097	8.24E-08	EAL domain-containing protein
VP1881	<i>tdpA</i>	7.3293	3.15E-16	EAL domain-containing protein
VP2366		2.5829	8.18E-07	sensor domain-containing diguanylate cyclase
VP2446		2.0804	9.12E-10	bifunctional diguanylate cyclase/phosphodiesterase
VPA0202	<i>gefA</i>	2.3941	1.38E-10	GGDEF domain-containing protein
VPA0360	<i>scrM</i>	3.1038	1.11E-07	GGDEF domain-containing protein
VPA0737		0.4175	9.87E-08	EAL domain-containing response regulator
VPA0818		3.2724	1.78E-17	EAL domain-containing protein
VPA0927		2.1620	2.77E-07	diguanylate cyclase
VPA1104		2.1720	9.15E-12	EAL domain-containing protein
VPA1324	<i>vopY</i>	0.0111	4.67E-12	EAL domain-containing protein
VPA1429		3.9877	1.31E-11	EAL domain-containing protein
VPA1457		2.1180	9.28E-05	GGDEF domain-containing protein
VPA1511	<i>scrC</i>	0.3978	2.55E-25	bifunctional diguanylate cyclase/phosphodiesterase
VPA1547	<i>lafV</i>	4.9611	5.20E-35	EAL domain-containing protein
Polar flagellum				
VP0770	<i>flgN</i>	2.0972	1.02E-10	flagellar export chaperone FlgN
VP0771	<i>flgM</i>	2.7996	1.95E-14	flagellar biosynthesis anti-sigma factor FlgM
VP0773		2.2715	7.74E-14	chemotaxis protein CheV
VP0782	<i>flgH</i>	0.4676	2.01E-05	flagellar basal body L-ring protein FlgH
VP0783		0.4845	6.67E-06	flagellar basal body P-ring protein FlgI
VP0784	<i>flgJ</i>	0.4245	2.35E-08	flagellar assembly peptidoglycan hydrolase FlgJ
VP0786	<i>flgL</i>	0.2722	1.74E-17	flagellar hook-associated protein FlgL
VP0790		7.9988	4.04E-103	flagellin
VP0791		6.2601	7.03E-13	flagellin
VP2230		2.5554	8.70E-11	protein phosphatase CheZ
VP2236	<i>flhB</i>	0.4606	5.39E-12	flagellar biosynthesis protein FlhB
VP2237	<i>flhR</i>	0.4531	1.44E-19	flagellar biosynthetic protein FlhR
VP2254	<i>flhS</i>	3.7418	3.03E-24	flagellar export chaperone FlhS
VP2256	<i>flhD</i>	3.0864	9.49E-27	flagellar filament capping protein FlhD
VP2257	<i>flaG</i>	4.1666	6.62E-22	flagellar protein FlaG
VP2258		6.8022	9.85E-43	flagellin
VP2259		7.1433	5.16E-67	flagellin
VP2261		3.9356	1.11E-23	flagellin
VP2811		6.0992	1.45E-46	tetratricopeptide repeat protein
Lateral flagella				
VPA0266	<i>flgD</i>	0.2705	1.97E-07	flagellar hook assembly protein FlgD
VPA0267	<i>flgE</i>	0.2780	1.09E-13	flagellar hook protein FlgE
VPA0268		0.2538	3.28E-10	flagellar basal body rod protein FlgF

Table 1 (continued)

Gene ID	Name	Fold change	pValue	Products
VPA0269	<i>flgG</i>	0.2620	7.41E-08	flagellar basal-body rod protein FlgG
VPA0270	<i>flgH</i>	0.3546	0.000178328	flagellar basal body L-ring protein FlgH
VPA0271		0.4428	0.000105137	flagellar basal body P-ring protein FlgI
VPA0272		0.4806	0.001117866	rod-binding protein
VPA0273	<i>flgK</i>	0.3282	7.50E-11	flagellar hook-associated protein FlgK
VPA0274	<i>flgL</i>	0.4612	7.22E-07	flagellar hook-associated protein FlgL
VPA0275		0.4693	2.46E-10	flagellin
VPA1532	<i>flhJ</i>	0.2382	4.90E-05	flagellar export protein FlhJ
VPA1533	<i>flhI</i>	0.2939	2.96E-15	flagellar protein export ATPase FlhI
VPA1534	<i>flhH</i>	0.2049	3.39E-10	flagellar assembly protein FlhH
VPA1535		0.3093	9.50E-12	flagellar motor switch protein FlhG
VPA1540		3.7989	0.001433368	flagellar motor switch protein FlhM
VPA1546	<i>flhA</i>	2.8816	2.99E-14	flagellar biosynthesis protein FlhA
VPA1550	<i>flhD</i>	0.5724	0.015457347	flagellar filament capping protein FlhD
VPA1551	<i>flhS</i>	0.4815	0.009563735	flagellar export chaperone FlhS
VPA1553		0.4708	7.03E-05	flagellar hook-length control protein FlhK
VPA1555	<i>lafS</i>	0.4711	0.002745437	lateral flagellar system RNA polymerase sigma factor LafS
CPS				
VP0216		2.1553	2.06E-12	capsule biosynthesis GfcC family protein
VP0217		2.6809	1.37E-15	YjbF family lipoprotein
VP0220		0.4688	5.12E-36	SLBB domain-containing protein
EPS				
VP1462	<i>scvL</i>	0.4283	0.000255339	chain-length determining protein
VP1464	<i>scvJ</i>	0.3847	8.15E-05	O-antigen ligase family protein
VP1465	<i>scvI</i>	0.3512	1.55E-05	lipopolysaccharide biosynthesis protein
VP1466	<i>scvH</i>	0.2622	5.74E-07	glycosyltransferase family 4 protein
VPA1403	<i>cpsA</i>	0.1401	5.32E-16	undecaprenyl-phosphate glucose phosphotransferase
VPA1404	<i>cpsB</i>	0.0700	4.92E-25	outer membrane beta-barrel protein
VPA1405	<i>cpsC</i>	0.0874	4.96E-12	polysaccharide biosynthesis/export family protein
VPA1406	<i>cpsD</i>	0.1361	1.38E-19	polysaccharide biosynthesis tyrosine autokinase
VPA1407	<i>cpsE</i>	0.1120	1.09E-16	putative capsular polysaccharide synthesis family protein
VPA1408	<i>cpsF</i>	0.1806	2.05E-15	glycosyltransferase
VPA1409	<i>cpsG</i>	0.1575	7.79E-12	O-antigen ligase family protein
VPA1410	<i>cpsH</i>	0.2847	1.13E-08	putative capsular polysaccharide synthesis family protein
VPA1411	<i>cpsI</i>	0.3166	1.74E-11	glycosyltransferase
VPA1412	<i>cpsJ</i>	0.3063	1.56E-09	oligosaccharide flippase family protein
VPA1413	<i>cpsK</i>	0.3171	0.000623289	VanZ family protein
T3SS1				
VP1656	<i>vopD</i>	0.4882	2.66E-16	type III secretion system translocon subunit VopD
VP1657	<i>vopB</i>	0.4328	9.53E-26	type III secretion system translocon subunit VopB
T3SS2				
VPA1321	<i>vopC</i>	0.4083	1.06E-13	T3SS2 effector GTPase-activating deamidase VopC
VPA1322		0.4576	2.65E-09	hypothetical protein
VPA1327	<i>vopT</i>	0.2788	1.10E-07	T3SS effector ADP-ribosyltransferase toxin VopT
VPA1328		0.1617	1.14E-06	hypothetical protein

(continued on next page)

Table 1 (continued)

Gene ID	Name	Fold change	pValue	Products
VPA1329		0.0697	5.76E-23	conjugal transfer protein TraA
VPA1331		0.0957	8.31E-18	VPA1331 family putative T3SS effector
VPA1332	<i>vtrA</i>	2.7526	2.62E-08	type III secretion system transcriptional regulator VtrA
VPA1334		0.2045	2.02E-17	hypothetical protein
VPA1335		0.2520	7.85E-10	flagellar biosynthetic protein FliQ
VPA1336	<i>vopZ</i>	0.1798	1.88E-23	type III secretion system effector VopZ
VPA1337		0.2637	6.23E-08	VPA1337 family putative T3SS effector
VPA1338		0.1669	3.53E-31	type III secretion system ATPase
VPA1339		0.0731	4.01E-55	secretin N-terminal domain-containing protein
VPA1340		0.0124	2.17E-46	VPA1340 family putative T3SS effector
VPA1341		0.0084	2.17E-30	hypothetical protein
VPA1342		0.0080	6.75E-44	EscR/YscR/HrcR family type III secretion system export apparatus protein
VPA1343		0.0185	6.19E-45	hypothetical protein
VPA1345		0.1035	8.34E-70	hypothetical protein
VPA1346	<i>vopA</i>	0.0377	7.77E-83	type III secretion system YopJ family effector VopA
VPA1348	<i>vtrB</i>	0.2245	5.17E-10	winged helix-turn-helix domain-containing protein
VPA1349		0.0950	2.18E-46	FliM/FliN family flagellar motor C-terminal domain-containing protein
VPA1350		0.0840	7.34E-59	VPA1350 family putative T3SS effector
VPA1351		0.0712	2.99E-66	VPA1351 family putative T3SS effector
VPA1352		0.0996	2.80E-24	VPA1352 family putative T3SS effector
VPA1353		0.0726	5.73E-62	OmpA family protein
VPA1354		0.0421	6.53E-37	EscU/YscU/HrcU family type III secretion system export apparatus switch protein
VPA1355		0.0542	3.01E-66	FHIPEP family type III secretion protein
VPA1356		0.0324	2.10E-43	hypothetical protein
VPA1357		0.0948	4.81E-45	hypothetical protein
VPA1358		0.0877	7.30E-15	dimethyladenosine transferase
VPA1359		0.0741	1.68E-19	hypothetical protein
VPA1360		0.0596	1.15E-33	hypothetical protein
VPA1361	<i>vopD2</i>	0.0612	1.19E-69	type III secretion system translocator protein VopD2
VPA1362	<i>vopB2</i>	0.0203	2.50E-126	type III secretion system translocator protein VopB2
VPA1363		0.0265	4.73E-27	molecular chaperone
VPA1364		0.0365	1.06E-30	hypothetical protein
VPA1365		0.0355	9.56E-59	hypothetical protein
VPA1366		0.0313	2.45E-37	hypothetical protein
VPA1367		0.0182	2.28E-77	type III secretion protein
VPA1368		0.0106	3.78E-61	hypothetical protein
VPA1369		0.3862	1.95E-10	hypothetical protein
VPA1370	<i>vopL</i>	0.0687	4.51E-75	type III secretion system effector VopL
TDH				
VPA1314	<i>tdh2</i>	0.0959	4.66E-129	thermostable direct hemolysin TDH
T6SS1				
VP1393	<i>hcp 1</i>	0.4367	3.02E-11	Hcp family type VI secretion system effector
VP1398		0.4718	3.42E-09	DUF2169 domain-containing protein
VP1399		0.4426	3.55E-08	hypothetical protein
VP1400		0.4289	8.36E-05	protein kinase family protein
VP1401	<i>tssA</i>	0.2730	5.02E-19	type VI secretion system protein TssA

Table 1 (continued)

Gene ID	Name	Fold change	pValue	Products
VP1402	<i>tssB</i>	0.3808	1.16E-11	type VI secretion system contractile sheath small subunit
VP1403	<i>tssC</i>	0.4499	2.39E-16	type VI secretion system contractile sheath large subunit
VP1411		0.3367	1.35E-05	FHA domain-containing protein
VP1412	<i>tssJ</i>	0.1422	2.86E-05	type VI secretion system lipoprotein TssJ
VP1413	<i>tssK</i>	0.1849	4.15E-17	type VI secretion system baseplate subunit TssK
VP1414	<i>icmH</i>	0.1483	6.56E-10	type IVB secretion system protein IcmH/DotU
T6SS2				
VPA1024		0.2664	1.17E-15	hypothetical protein
VPA1025		0.4598	2.41E-05	PAAR domain-containing protein
VPA1027	<i>hcp 2</i>	0.2351	6.16E-27	type VI secretion system tube protein Hcp
VPA1028	<i>tssH</i>	0.4740	8.53E-14	type VI secretion system ATPase TssH
VPA1029	<i>tssG</i>	0.3195	1.33E-11	type VI secretion system baseplate subunit TssG
VPA1030	<i>tssF</i>	0.4058	5.11E-12	type VI secretion system baseplate subunit TssF
VPA1031	<i>tssE</i>	0.2866	1.25E-07	type VI secretion system baseplate subunit TssE
VPA1032		0.4209	3.68E-05	type VI secretion system accessory protein TagJ
VPA1033	<i>tssC</i>	0.2607	7.88E-15	type VI secretion system contractile sheath large subunit
VPA1034	<i>tssC</i>	0.2337	2.01E-16	type VI secretion system contractile sheath large subunit
VPA1035	<i>tssB</i>	0.3139	5.53E-14	type VI secretion system contractile sheath small subunit
VPA1036	<i>tssA</i>	0.1932	1.30E-32	type VI secretion system protein TssA
VPA1037		0.1727	1.12E-22	protein phosphatase 2C domain-containing protein
VPA1038	<i>tagF</i>	0.1150	1.74E-30	type VI secretion system-associated protein TagF
VPA1039	<i>tssM</i>	0.0575	2.89E-48	type VI secretion system membrane subunit TssM
VPA1040	<i>tssL</i>	0.0334	1.20E-67	type VI secretion system protein TssL, long form
VPA1041	<i>tssK</i>	0.0369	5.27E-65	type VI secretion system baseplate subunit TssK
VPA1042	<i>tssJ</i>	0.0621	1.66E-36	type VI secretion system lipoprotein TssJ
VPA1043	<i>tagH</i>	0.1915	8.00E-26	type VI secretion system-associated FHA domain protein
VPA1044		0.1124	6.54E-29	TagH serine/threonine-protein kinase
Putative regulators				
VP0072	<i>asnC</i>	4.0687	2.25E-25	transcriptional regulator AsnC
VP0247	<i>rraA</i>	3.0138	1.78E-20	ribonuclease E activity regulator RraA
VP0252	<i>cytR</i>	3.9133	1.01E-11	DNA-binding transcriptional regulator CytR
VP0289		2.6271	5.52E-08	Crp/Fnr family transcriptional regulator
VP0324	<i>argR</i>	2.9194	5.82E-21	transcriptional regulator ArgR
VP0355		2.1992	0.000236745	GntR family transcriptional regulator
VP0358	<i>scrO</i>	3.3804	9.33E-08	DeoR family transcriptional regulator
VP0403		2.0556	0.000937852	helix-turn-helix domain-containing protein
VP0475		2.6049	2.27E-09	LysR family transcriptional regulator

(continued on next page)

Table 1 (continued)

Gene ID	Name	Fold change	pValue	Products
VP0553	<i>trpR</i>	0.4319	5.77E-13	<i>trp</i> operon repressor
VP0595	<i>iscR</i>	0.3124	2.03E-21	Fe-S cluster assembly transcriptional regulator <i>IscR</i>
VP0635		2.1355	4.42E-06	LysR family transcriptional regulator
VP0713		2.1219	2.24E-06	winged helix-turn-helix domain-containing protein
VP0833	<i>fcxX</i>	2.3715	3.23E-08	ferric iron uptake transcriptional regulator <i>FcxX</i>
VP0838	<i>seqA</i>	2.1114	2.12E-09	replication initiation negative regulator <i>SeqA</i>
VP1101	<i>cysB</i>	10.4660	3.31E-86	HTH-type transcriptional regulator <i>CysB</i>
VP1104	<i>lrp</i>	2.4327	3.98E-07	leucine-responsive transcriptional regulator <i>Lrp</i>
VP1202		4.5168	2.98E-06	response regulator
VP1212		0.2359	3.69E-63	response regulator transcription factor
VP1244		2.8668	1.14E-14	response regulator
VP1328		3.4624	4.36E-18	GntR family transcriptional regulator
VP1376		5.2689	1.18E-20	response regulator
VP1379		2.1925	2.94E-05	LysE family translocator
VP1482		2.0011	1.76E-08	response regulator
VP1502		3.9330	1.30E-29	sigma-54 dependent transcriptional regulator
VP1649		2.2445	0.000928068	GntR family transcriptional regulator
VP1763		2.4738	9.83E-11	MarR family transcriptional regulator
VP1778	<i>puuR</i>	2.2900	3.54E-09	HTH-type transcriptional regulator <i>PuuR</i>
VP1962		2.6280	6.00E-13	Crp/Fnr family transcriptional regulator
VP1993		0.3317	2.28E-23	helix-turn-helix domain-containing protein
VP2009		3.4881	3.15E-08	response regulator
VP2266		5.8838	1.14E-12	helix-turn-helix domain-containing protein
VP2402	<i>ebgR</i>	2.2454	4.37E-09	transcriptional regulator <i>EbgR</i>
VP2478		2.6976	7.25E-12	response regulator
VP2516	<i>opaR</i>	2.9274	0.000122252	transcriptional regulator <i>OpaR</i>
VP2546	<i>csrA</i>	2.2577	4.83E-08	carbon storage regulator <i>CsrA</i>
VP2603		0.4863	3.34E-06	LysR family transcriptional regulator
VP2752	<i>oxyR</i>	2.7041	5.88E-19	DNA-binding transcriptional regulator <i>OxyR</i>
VP2777		2.1875	9.87E-08	transcriptional regulator
VP2808	<i>nsrR</i>	2.8367	1.47E-14	nitric oxide-sensing transcriptional repressor <i>NsrR</i>
VP2836		3.3989	2.77E-24	TetR/AcrR family transcriptional regulator
VP2866		2.5429	6.47E-12	response regulator transcription factor
VP2893	<i>cadC</i>	2.9844	5.56E-11	lysine decarboxylation/transport transcriptional activator <i>CadC</i>
VP2941	<i>fabR</i>	2.1154	5.70E-08	HTH-type transcriptional repressor <i>FabR</i>
VP2945	<i>lexA</i>	3.2597	4.58E-18	transcriptional repressor <i>LexA</i>
VPA0034		2.2253	9.54E-06	GntR family transcriptional regulator
VPA0091		6.0795	4.14E-10	Lrp/AsnC family transcriptional regulator
VPA0240	<i>phnR</i>	2.2712	5.72E-09	phosphonate utilization transcriptional regulator <i>PhnR</i>
VPA0290		2.1339	8.85E-06	LysR family transcriptional regulator
VPA0303		2.0666	8.37E-07	DNA-binding transcriptional regulator <i>YciT</i>
VPA0358		3.4696	4.96E-06	LuxR C-terminal-related transcriptional regulator
VPA0359		2.8044	0.000286264	helix-turn-helix transcriptional regulator

Table 1 (continued)

Gene ID	Name	Fold change	pValue	Products
VPA0376		2.0061	0.002389784	LysR family transcriptional regulator
VPA0381		2.0732	0.000752165	AraC family transcriptional regulator
VPA0387		2.0932	0.000938405	LysR family transcriptional regulator
VPA0497		4.5187	2.12E-06	winged helix-turn-helix domain-containing protein
VPA0507		0.2998	0.00450362	helix-turn-helix transcriptional regulator
VPA0519		2.0168	0.000373655	LysR family transcriptional regulator
VPA0602		2.4069	0.000602175	LysR family transcriptional regulator
VPA0641		2.6863	7.96E-15	LysR family transcriptional regulator
VPA0662	<i>cueR</i>	2.2624	2.05E-06	Cu(I)-responsive transcriptional regulator
VPA0675	<i>torS</i>	2.0955	2.65E-07	TMAO reductase system sensor histidine kinase/response regulator <i>TorS</i>
VPA0717		0.3710	3.79E-09	LysR family transcriptional regulator
VPA0734		2.6364	3.55E-07	LysR family transcriptional regulator
VPA0804		2.0492	1.45E-05	XRE family transcriptional regulator
VPA0910		0.2782	1.68E-05	helix-turn-helix transcriptional regulator
VPA0938		2.4216	0.000174609	AraC family transcriptional regulator
VPA0961		5.7693	6.36E-08	LysR family transcriptional regulator
VPA0964	<i>uhpA</i>	2.6727	1.52E-05	transcriptional regulator <i>UhpA</i>
VPA0988	<i>rnk</i>	0.3422	1.28E-12	nucleoside diphosphate kinase regulator
VPA1052		3.0187	1.70E-09	TetR/AcrR family transcriptional regulator
VPA1164		2.4047	0.003055969	helix-turn-helix transcriptional regulator
VPA1195		2.6117	1.30E-15	response regulator
VPA1276		2.3720	3.77E-10	response regulator
VPA1332	<i>vtrA</i>	2.7526	2.62E-08	type III secretion system transcriptional regulator <i>VtrA</i>
VPA1516		2.8429	0.000623385	response regulator transcription factor
VPA1589		2.0828	3.11E-06	LysR family transcriptional regulator
VPA1592		3.3071	2.55E-21	AraC family transcriptional regulator
VPA1607		2.2799	0.002286431	LysR family transcriptional regulator
VPA1623	<i>malT</i>	0.3062	2.72E-16	HTH-type transcriptional regulator <i>MalT</i>
VPA1636		6.3637	9.70E-36	helix-turn-helix transcriptional regulator
VPA1665		2.7364	5.82E-11	response regulator transcription factor
VPA1732		3.8065	2.81E-19	response regulator transcription factor

swimming motility while inhibited swarming motility of *V. parahaemolyticus*.

Previous studies have shown that Mg^{2+} affected flagellar gene expression and motility of *Vibrio* species. For example, Mg^{2+} supported the swarming motility of *V. alginolyticus* at temperatures below 28 °C [27]. In addition, Mg^{2+} induced the biosynthesis of flagella and motility of *V. fischeri* via the signaling pathway composed of two diguanylate cyclases, MifA and MifB, and also the sugar phosphotransferase system [29,53]. Mg^{2+} also promoted the motility of several other *Vibrio* species including *V. splendidus*, *V. parahaemolyticus*, and *V. anguillarum* [28]. The data presented here showed that Mg^{2+} not only affected the swimming

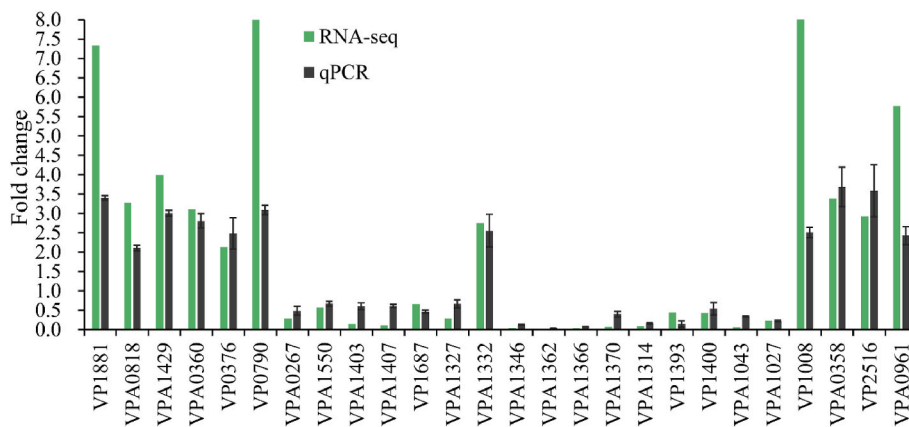


Fig. 3. Validation of RNA-seq by qPCR. The relative mRNA levels of each target gene were compared between 0 and 55 mM Mg^{2+} . The expression level of 16S rRNA gene was used as the internal control.

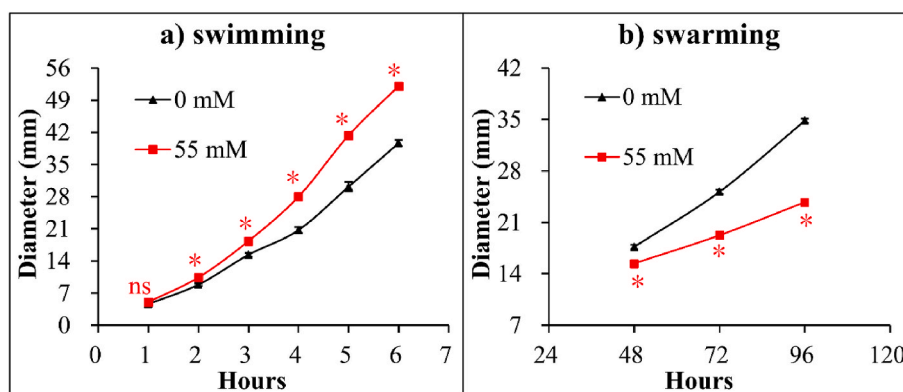


Fig. 4. Regulation of swimming and swarming motility of *V. parahaemolyticus* by Mg^{2+} . Swimming (a) or swarming (b) motility of *V. parahaemolyticus* in different concentrations of Mg^{2+} were detected by measuring the diameters of swimming or swarming areas in semi-solid swimming or on swarming agar plates. The data at each time point are expressed as the mean \pm SD of three independent experiments with at least three replicates each. *, $P < 0.05$. ns, $P > 0.05$.

and swarming motility but also the gene expression of both two flagellar systems. Flagellar gene expression in *V. parahaemolyticus* is strictly regulated by various factors, including regulators such as ToxR [54], LafK [55], H-NS [56] and CalR [57], chemicals such as chloramphenicol [44] and L-arabinose [44], and different biological behavior processes such as biofilm formation [36] and EPS phase variation [44]. The resented data further enriched the regulatory networks of flagellar genes in *V. parahaemolyticus*.

3.5. Biofilm-related DEGs

Mg^{2+} plays a critical role in biofilm architecture of *Pseudomonas mendocina* and enhances biofilm formation by *P. fluorescens* and *Listeria monocytogenes* [58–60]. By contrast, Mg^{2+} decreases biofilm formation by *Bacillus* species by regulating matrix gene expression and EPS production [61,62]. In addition, Mg^{2+} significantly reduces the total biofilm biomass of *Acidithiobacillus ferrooxidans* in a dose-dependent manner [63]. Moreover, Mg^{2+} limitation increases aggregation, EPS production and biofilm formation by *P. aeruginosa* [64]. These observations motivated us to detect whether Mg^{2+} has regulatory effect on biofilm formation by *V. parahaemolyticus*. As demonstrated by the CV staining assay (Fig. 5a), the relative biofilm produced by *V. parahaemolyticus* grown under the condition with additional Mg^{2+} was significantly less than that grown under the condition without additional Mg^{2+} . The colony morphology assays further showed that *V. parahaemolyticus* formed wrinkled colonies on the HI plate but smooth colonies on the HI plate supplemented with 55 mM $MgCl_2$ (Fig. 5b). These results suggested that

Mg^{2+} inhibits biofilm formation by *V. parahaemolyticus*.

EPS is a major component of the biofilm matrix [15]. The *cps* and *scv* gene loci are demonstrated to contribute to EPS production in *V. parahaemolyticus* [16]. In this work, the data showed that all the *cps* genes (*cpsA-K*) and four *scv* genes were significantly downregulated by Mg^{2+} (Table 1). Although both the *cps* and *scv* gene loci are involved in the synthesis of EPS and biofilm formation, but only the *cps* gene cluster affects the switching between wrinkled and smooth colony phenotype of *V. parahaemolyticus* [16,36], indicating that the *cps* gene cluster may contribute more to EPS synthesis.

The c-di-GMP signal can posttranscriptionally regulate cellular pathways such as biofilm formation, motility, and virulence gene expression. An increase in the concentration of c-di-GMP molecules in bacterial cells enhances biofilm formation, but inhibits motility and virulence factors production [17]. In this study, the data showed that the intracellular c-di-GMP level of *V. parahaemolyticus* grown in 55 mM Mg^{2+} was much lower than that of bacteria grown in HI broth only, suggesting that additional Mg^{2+} inhibited the production of c-di-GMP in *V. parahaemolyticus* (Fig. 6). Furthermore, a total of 18 genes that are probably involved in c-di-GMP metabolism were significantly and differentially expressed in response to Mg^{2+} stimulation (Table 1). Of these, 15 were upregulated including *tdpA*, *gefA* and *lafV*, and 3 were downregulated including *vopY* and *scrC*. Roles of ScrC [19], GefA [24], LafV [22], TpdA [23] and VopY [25] have been documented in literature, showing that they are involved in motility and/or biofilm formation. However, roles of the other 13 putative c-di-GMP-related genes in cellular pathways such as c-di-GMP metabolism, motility and biofilm

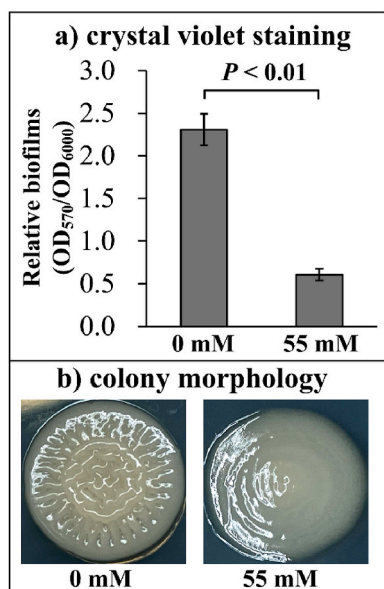


Fig. 5. Mg²⁺ inhibited biofilm formation by *V. parahaemolyticus*. Biofilm formation by *V. parahaemolyticus* were assessed by crystal violet staining (a) and colony morphology (b). Pictures are representative of three independent experiments with three replicates each. (For interpretation of the references to colour in this figure legend, the reader is referred to the Web version of this article.)

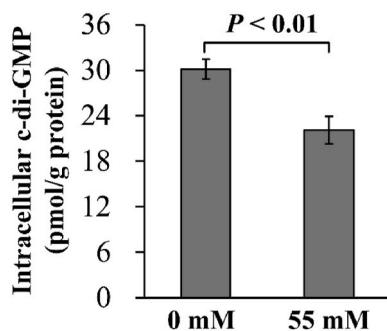


Fig. 6. Mg²⁺ decreased the intracellular c-di-GMP level of *V. parahaemolyticus*. *V. parahaemolyticus* was grown in HI broth containing 0 or 55 mM Mg²⁺ at 37 °C with shaking at 200 rpm in, and then harvested at an OD₆₀₀ value of 1.5. c-di-GMP was extracted by ultrasonication, and then was measured using a c-di-GMP Enzyme-linked Immunosorbent Assay (ELISA) Kit. Intracellular c-di-GMP level was expressed as pmol/g. The data are expressed as the mean ± SD of three independent experiments with three replicates each.

formation are still completely unknown. Clarifying the roles of these genes will help us to understand the regulatory mechanisms of Mg²⁺ on c-di-GMP synthesis and biofilm formation of *V. parahaemolyticus*.

CPS contributes a negative role to biofilm formation in *Vibrio* species [10]. The RNA-seq data showed that the expression levels of 3 CPS-associated genes were significantly and differentially regulated by Mg²⁺ (Table 1). Two were upregulated (VP0216 and VP0217) and 1 was downregulated (VP0220). In addition, *V. parahaemolyticus* formed OP colonies on HI plates or HI plates containing 55 mM Mg²⁺ (Fig. 7), suggesting that Mg²⁺ had no regulatory effect on the production of CPS. *V. parahaemolyticus* undergoes phase variation between wrinkled and smooth colony phenotypes, and the wrinkled strain has stronger biofilm capacity than the smooth strain [36]. Chloramphenicol also has a negative effect on biofilm formation by *V. parahaemolyticus* [44]. However, neither the wrinkled and smooth colony variation nor chloramphenicol affects the CPS production of *V. parahaemolyticus* [36,44].

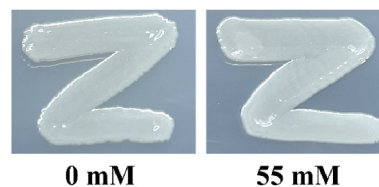


Fig. 7. Mg²⁺ did not affect CPS production of *V. parahaemolyticus*. *V. parahaemolyticus* was streaked onto a HI plate containing 0 or 55 mM Mg²⁺, and then incubated at 37 °C for 24 h. Pictures were representative of two independent experiments with three replicates each.

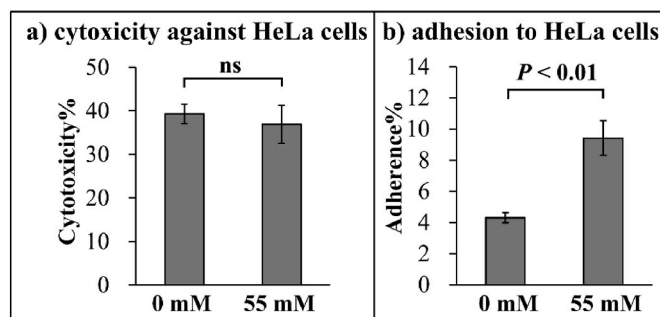


Fig. 8. Mg²⁺ enhanced the cell adherence activity of *V. parahaemolyticus*. The results were expressed as the mean ± SD from six replicates. **a) Cytotoxicity against HeLa cells.** The cytotoxicity of *V. parahaemolyticus* against HeLa cells was evaluated in terms the release of LDH. **b) Adherence to HeLa cells.** The percent adherence was calculated as bacterial cells adhered/input bacterial cells.

These observations suggest that CPS may not be the main influencer of biofilm formation by *V. parahaemolyticus*.

3.6. DEGs involved in the key virulence factors

V. parahaemolyticus RIMD2210633 produces multiple virulence factors, including T3SS1 (VP1656-1702), T3SS2 (VPA1320-1370), TDH (VPA1314 and VPA1378), T6SS1 (VP1386-1420) and T6SS2 (VPA1024-1046) [13]. Expression of 2 T3SS1-associated genes were significantly downregulated by Mg²⁺ (Table 1). The T3SS1 gene cluster harbors 47 coding genes, and controlling two of them may not effectively affect the secretion system's function. T3SS1 is responsible for the cytotoxicity of *V. parahaemolyticus* against HeLa cells [6]. To further confirm whether Mg²⁺ affects the expression of T3SS1, the cytotoxicity of *V. parahaemolyticus* against HeLa cells was measured herein. As shown in Fig. 8a, the cytotoxicity ability of *V. parahaemolyticus* grown in the Mg²⁺ condition was similar to that grown in the normal condition, indicating that Mg²⁺ had no effect on the expression of T3SS1 genes.

In *V. parahaemolyticus* RIMD2210633, the T3SS2 gene locus and the two copies of *tdh* genes are assembled on an 80 kb pathogenicity island (Vp-PAI) within chromosome II [13]. Expression of Vp-PAI genes is strongly induced by bile and the two transcriptional regulators, VtrA and VtrB [65]. VtrA and VtrC constitute a co-component signal transduction system that senses and binds bile acids and then induces *vtrB* transcription and other Vp-PAI gene expression [66,67]. The data presented here showed that the expression of 42 T3SS2 genes including *vtrA* and *tdh2* was differentially regulated by Mg²⁺ (Table 1). However, *vtrA* was upregulated while the other genes were downregulated by Mg²⁺. This phenomenon is contradictory and difficult to explain, and the underlying molecular mechanism needs to be further investigated. The *tdh2* gene is predominantly responsible for TDH activity in *V. parahaemolyticus* RIMD2210633 [2]. Therefore, the inhibition of *tdh2* expression by Mg²⁺ motivated us to detect whether the ion affects the hemolytic activity of *V. parahaemolyticus*. Unfortunately, the

Wagatsuma agar supplemented with 55 mM Mg^{2+} always spontaneously undergone hemolysis (data not shown), which was likely due to increased osmotic pressure in the agar caused by Mg^{2+} . Anyway, we were able to speculate that Mg^{2+} was very likely to inhibit the enterotoxicity and hemolytic activity of *V. parahaemolyticus*.

A total of 11 T6SS1 and 20 T6SS2 genes were downregulated by Mg^{2+} (Table 1), accounting for 31.4% (11/35) of the total T6SS1 genes and 87.0% (20/23) of the total T6SS2 genes, respectively. T6SS1 possesses anti-bacterial activity, while T6SS2 possesses cell adhesive activity [7,8]. We compared the differences in cell adherence of *V. parahaemolyticus* cultured under the conditions supplemented with 0 and 55 Mg^{2+} against HeLa cells. As shown in Fig. 8b, the adhesion rate of *V. parahaemolyticus* under the condition of 55 mM Mg^{2+} was approximately 10%, whereas the condition without Mg^{2+} was only about 4%. Therefore, Mg^{2+} induced the cell adherence of *V. parahaemolyticus*, which was independent of its regulation of T6SS2 expression. *V. parahaemolyticus* also express other adhesion factors, such as type IV pili and MAM-7 [4]. Further research is needed to determine whether these adhesion factors are related to Mg^{2+} -mediated adherence against to HeLa cells.

3.7. DEGs encode putative regulators

A total of 83 genes encoding putative regulators were differentially regulated by Mg^{2+} , including 73 upregulated genes and 10 downregulated genes (Table 1). Of these, 3 DEGs (VPA0381, VPA0938, and VPA1592) encode AraC family transcriptional regulators; 4 DEGs (VP0355, VP1328, VP1649 and VPA0034) encode GntR family transcriptional regulators; 14 DEGs including VPA0961 encode LysR family transcriptional regulators; 1 DEG (VP1763) encodes MarR family transcriptional regulator; 2 DEGs (VP2836 and VPA1052) encode TetR/AcrR family transcriptional regulators. Proteins belong to these family are global regulators that control multiple cellular pathways.

The expression level of *cysB* (VP1101) was upregulated 10.4660-fold by Mg^{2+} . In *V. fischeri*, CysB was shown to be required for the growth on sulfur sources and cysteine [68]. VPA0961, which was shown to be significantly affected by Na^+ concentration, L-arabinose and different stages of biofilm formation [44,44,69], was upregulated 5.7693-fold by Mg^{2+} . The expression levels of *opaR* (VP2516), *oxyR* (VP2752), *cadC* (VP2893) and *csrA* (VP2546) were all upregulated more than 2-fold by Mg^{2+} , suggesting that these regulators are likely be involved in adaptation to Mg^{2+} stress. OpaR is a master global regulator of QS that controls downstream gene transcription in response to changes in cell density [70]. Pathways regulated by OpaR include motility, biofilm formation and virulence gene expression [43,46,50,71]. OxyR, a redox-sensitive transcriptional regulator, is involved in oxidation resistance of *V. parahaemolyticus*, and also participates in the regulation of motility, biofilm formation and bacterial growth [72,73]. CadC regulates the transcription of more than 500 genes in the sub-lethal acidic conditions including the *cadBA* operon, which is involved in the acid tolerance response of *V. parahaemolyticus* [74]. CsrA promotes swarming but not swimming motility, and can regulates the carbon and nitrogen metabolism of *V. alginolyticus* [75]. Moreover, CsrA regulates 22% of the total genes of *V. cholerae*, including those involved in metabolism, iron uptake, and flagellar system [76]. In addition, *iscR* (VP0595) was downregulated 0.3124-fold by Mg^{2+} . In *V. vulnificus*, IscR was shown to be a global regulator that contributes to the expression of various virulence and survival genes, and was directly upregulated by Apha [77–79]. However, the functions of most other putative regulators are still completely unknown, and more research should be performed in the future to elucidate their roles in regulating gene expression in *V. parahaemolyticus*.

3.8. Conclusions and outlook

In conclusion, this work demonstrated that Mg^{2+} had a

comprehensive impact on the physiology and gene expression of *V. parahaemolyticus*. RNA-seq demonstrated that the expression of 1494 genes was significantly regulated by Mg^{2+} , accounting for about 30.9% of total genes of *V. parahaemolyticus* RIMD 2210633. Of these, 868 were upregulated, and 626 were downregulated. The majority of the genes associated with lateral flagella, EPS, T3SS2, T6SS1, T6SS2, and TDH were downregulated by Mg^{2+} . A total of 18 genes that may be involved in c-di-GMP metabolism were significantly differentially expressed in response to Mg^{2+} . More than 80 genes encoding putative regulators were also significantly and differentially regulated by Mg^{2+} , indicating that the adaptation process to Mg^{2+} stress may be strictly regulated by complex regulatory networks. In addition, Mg^{2+} promoted the growth, swimming motility and adhesion to HeLa cells of *V. parahaemolyticus*, but inhibited the swarming motility, biofilm formation, and c-di-GMP production. However, Mg^{2+} had no effect on CPS production and cytotoxicity against HeLa cells. The data in this work were beneficial for us to understand the regulatory roles of Mg^{2+} in the growth, behaviors, and gene expression of *V. parahaemolyticus*. It should be noted that this work only investigated the effects of Mg^{2+} close to the average in seawater on the behaviors and gene expression of *V. parahaemolyticus*. However, Mg^{2+} concentration in seawater is fluctuating and constantly changing, with some areas below or above the average concentration in seawater. Therefore, it is worth to investigate whether lower and higher Mg^{2+} concentrations have different effects on *V. parahaemolyticus*. In addition, the RNA-seq data were unable to reflect the dynamic response of *V. parahaemolyticus* to Mg^{2+} stimulation, as only logarithmic bacterial samples were collected, and more research should be further performed to uncover the molecular mechanisms in response to Mg^{2+} stress. Moreover, Mg^{2+} is widely distributed in human bodies, but 99% is contained in bone and soft tissue [80]. Mg^{2+} balance is maintained by the intestine and kidneys [80], and the Mg^{2+} content in the intestine is greatly influenced by dietary composition. Therefore, the role of Mg^{2+} in the intestinal infection and pathogenesis of *V. parahaemolyticus* deserves further research.

CRedit authorship contribution statement

Xue Li: Writing – original draft, Investigation, Funding acquisition, Formal analysis. **Xiaobai Zhang:** Writing – original draft, Investigation, Formal analysis. **Miaomiao Zhang:** Investigation. **Xi Luo:** Investigation. **Tingting Zhang:** Investigation. **Xianjin Liu:** Writing – review & editing, Validation, Supervision, Resources, Formal analysis. **Renfei Lu:** Writing – review & editing, Validation, Supervision, Resources, Project administration, Methodology, Funding acquisition. **Yiquan Zhang:** Writing – review & editing, Writing – original draft, Validation, Supervision, Methodology, Formal analysis, Conceptualization.

Declaration of competing interest

The authors declare that they have no known competing financial interests or personal relationships that could have appeared to influence the work reported in this paper.

Data availability

The original data presented in the study are included in the article/supplementary materials, further inquiries can be directed to the corresponding authors. The raw data of RNA-seq are deposited in the NCBI repository (accession number PRJNA1035152).

Acknowledgements

This work was supported by the Special Project on Clinical Medicine of Nantong University (2022JZ010) and the Research Project of Nantong Health Commission (QN2022044).

Appendix A. Supplementary data

Supplementary data to this article can be found online at <https://doi.org/10.1016/j.biofilm.2024.100194>.

References

- [1] Li YJ, Yang YF, Zhou YJ, Zhang RH, Liu CW, Liu H, et al. Estimating the burden of foodborne gastroenteritis due to nontyphoidal *Salmonella enterica*, *Shigella* and *Vibrio parahaemolyticus* in China. *PLoS One* 2022;17:e0277203.
- [2] Cai Q, Zhang Y. Structure, function and regulation of the thermostable direct hemolysin (TDH) in pandemic *Vibrio parahaemolyticus*. *Microb Pathog* 2018;123:242–5.
- [3] Osei-Adjei G, Huang X, Zhang Y. The extracellular proteases produced by *Vibrio parahaemolyticus*. *World J Microbiol Biotechnol* 2018;34:68.
- [4] Li L, Meng H, Gu D, Li Y, Jia M. Molecular mechanisms of *Vibrio parahaemolyticus* pathogenesis. *Microbiol Res* 2019;222:43–51.
- [5] Kodama T, Hiyoshi H, Okada R, Matsuda S, Gotoh K, Iida T. Regulation of *Vibrio parahaemolyticus* T3SS2 gene expression and function of T3SS2 effectors that modulate actin cytoskeleton. *Cell Microbiol* 2015;17:183–90.
- [6] Hiyoshi H, Kodama T, Iida T, Honda T. Contribution of *Vibrio parahaemolyticus* virulence factors to cytotoxicity, enterotoxigenicity, and lethality in mice. *Infect Immun* 2010;78:1772–80.
- [7] Salomon D, Gonzalez H, Updegraff BL, Orth K. *Vibrio parahaemolyticus* type VI secretion system 1 is activated in marine conditions to target bacteria, and is differentially regulated from system 2. *PLoS One* 2013;8:e61086.
- [8] Yu Y, Yang H, Li J, Zhang P, Wu B, Zhu B, et al. Putative type VI secretion systems of *Vibrio parahaemolyticus* contribute to adhesion to cultured cell monolayers. *Arch Microbiol* 2012;194:827–35.
- [9] Ashrafudoulla M, Mizan MFR, Park SH, Ha SD. Current and future perspectives for controlling *Vibrio* biofilms in the seafood industry: a comprehensive review. *Crit Rev Food Sci Nutr* 2021;61:1827–51.
- [10] Yildiz FH, Visick KL. *Vibrio* biofilms: so much the same yet so different. *Trends Microbiol* 2009;17:109–18.
- [11] McCarter LL. Dual flagellar systems enable motility under different circumstances. *J Mol Microbiol Biotechnol* 2004;7:18–29.
- [12] Enos-Berlage JL, Guvener ZT, Keenan CE, McCarter LL. Genetic determinants of biofilm development of opaque and translucent *Vibrio parahaemolyticus*. *Mol Microbiol* 2005;55:1160–82.
- [13] Makino K, Oshima K, Kurokawa K, Yokoyama K, Uda T, Tagomori K, et al. Genome sequence of *Vibrio parahaemolyticus*: a pathogenic mechanism distinct from that of *V. cholerae*. *Lancet* 2003;361:743–9.
- [14] Shime-Hattori A, Iida T, Arita M, Park KS, Kodama T, Honda T. Two type IV pili of *Vibrio parahaemolyticus* play different roles in biofilm formation. *FEMS Microbiol Lett* 2006;264:89–97.
- [15] Flemming HC, Wingender J. The biofilm matrix. *Nat Rev Microbiol* 2010;8:623–33.
- [16] Liu M, Nie H, Luo X, Yang S, Chen H, Cai P. A polysaccharide biosynthesis locus in *Vibrio parahaemolyticus* important for biofilm formation has homologs widely distributed in aquatic bacteria mainly from gammaproteobacteria. *mSystems* 2022;7:e0122621.
- [17] Mills E, Pultz IS, Kulasekara HD, Miller SI. The bacterial second messenger c-di-GMP: mechanisms of signalling. *Cell Microbiol* 2011;13:1122–9.
- [18] Romling U, Galperin MY, Gomelsky M. Cyclic di-GMP: the first 25 years of a universal bacterial second messenger. *Microbiol Mol Biol Rev* 2013;77:1–52.
- [19] Boles BR, McCarter LL. *Vibrio parahaemolyticus* scrABC, a novel operon affecting swarming and capsular polysaccharide regulation. *J Bacteriol* 2002;184:5946–54.
- [20] Kim YK, McCarter LL. ScrG, a GGDEF-EAL protein, participates in regulating swarming and sticking in *Vibrio parahaemolyticus*. *J Bacteriol* 2007;189:4094–107.
- [21] Kimbrough JH, Cribbs JT, McCarter LL. Homologous c-di-GMP-binding transcription factors orchestrate biofilm development in *Vibrio parahaemolyticus*. *J Bacteriol* 2020;202.
- [22] Kimbrough JH, McCarter LL. Identification of three new GGDEF and EAL domain-containing proteins participating in the scr surface colonization regulatory network in *Vibrio parahaemolyticus*. *J Bacteriol* 2021;203.
- [23] Martinez-Mendez R, Camacho-Hernandez DA, Sulvaran-Guel E, Zamorano-Sanchez D. A trigger phosphodiesterase modulates the global c-di-GMP pool, motility, and biofilm formation in *Vibrio parahaemolyticus*. *J Bacteriol* 2021;203:e0004621.
- [24] Zhong X, Lu Z, Wang F, Yao N, Shi M, Yang M. Characterization of GefA, a GGDEF domain-containing protein that modulates *Vibrio parahaemolyticus* motility, biofilm formation, and virulence. *Appl Environ Microbiol* 2022;88:e0223921.
- [25] Wu X, Zhou L, Ye C, Zha Z, Li C, Feng C, et al. Destruction of self-derived PAMP via T3SS2 effector VopY to subvert PAMP-triggered immunity mediates *Vibrio parahaemolyticus* pathogenicity. *Cell Rep* 2023;42:113261.
- [26] Islam Z, Hayashi N, Yamamoto Y, Doi H, Romero MF, Hirose S, Kato A. Identification and proximal tubular localization of the Mg(2+)-transporter, Slc41a1, in a seawater fish. *Am J Physiol Regul Integr Comp Physiol* 2013;305:R385–96.
- [27] Ulitzur S. Effect of temperature, salts, pH, and other factors on the development of peritrichous flagella in *Vibrio alginolyticus*. *Arch Microbiol* 1975;104:285–8.
- [28] O'Shea TM, Deloney-Marino CR, Shibata S, Aizawa S, Wolfe AJ, Visick KL. Magnesium promotes flagellation of *Vibrio fischeri*. *J Bacteriol* 2005;187:2058–65.
- [29] O'Shea TM, Klein AH, Geszvain K, Wolfe AJ, Visick KL. Diguanylate cyclases control magnesium-dependent motility of *Vibrio fischeri*. *J Bacteriol* 2006;188:8196–205.
- [30] Shrestha P, Razvi A, Fung BL, Eichinger SJ, Visick KL. Mutational analysis of *Vibrio fischeri* c-di-GMP-Modulating genes reveals complex regulation of motility. *J Bacteriol* 2022;204:e0010922.
- [31] Heinis JJ, Beuchat LR, Jones WK. Growth of heat-injured *Vibrio parahaemolyticus* in media supplemented with various cations. *Appl Environ Microbiol* 1977;33:1079–84.
- [32] Heinis JJ, Beuchat LR, Boswell FC. Antimetabolite sensitivity and magnesium uptake by thermally stressed *Vibrio parahaemolyticus*. *Appl Environ Microbiol* 1978;35:1035–40.
- [33] Bhattacharya M, Roy SS, Biswas D, Kumar R. Effect of Mg(2+) ion in protein secretion by magnesium-resistant strains of *Pseudomonas aeruginosa* and *Vibrio parahaemolyticus* isolated from the coastal water of Haldia port. *FEMS Microbiol Lett* 2000;185:151–6.
- [34] Sarty D, Baker NT, Thomson EL, Rafuse C, Ebanks RO, Graham LL, Thomas NA. Characterization of the type III secretion associated low calcium response genes of *Vibrio parahaemolyticus* RIMD2210633. *Can J Microbiol* 2012;58:1306–15.
- [35] Tiruvayipati S, Bhasu S. Host, pathogen and environment: a bacterial gbpA gene expression study in response to magnesium environment and presence of prawn carapace and commercial chitin. *Gut Pathog* 2016;8:23.
- [36] Wu Q, Li X, Zhang T, Zhang M, Xue X, Yang W, et al. Transcriptomic analysis of *Vibrio parahaemolyticus* underlying the wrinkly and smooth phenotypes. *Microbiol Spectr* 2022;10:e0218822.
- [37] Bray NL, Pimentel H, Melsted P, Pachter L. Near-optimal probabilistic RNA-seq quantification. *Nat Biotechnol* 2016;34:525–7.
- [38] Anders S, Huber W. Differential expression analysis for sequence count data. *Genome Biol* 2010;11:R106.
- [39] Kanehisa M, Goto S. KEGG: kyoto encyclopedia of genes and genomes. *Nucleic Acids Res* 2000;28:27–30.
- [40] Tatusov RL, Galperin MY, Natale DA, Koonin EV. The COG database: a tool for genome-scale analysis of protein functions and evolution. *Nucleic Acids Res* 2000;28:33–6.
- [41] Harris MA, Clark J, Ireland A, Lomax J, Ashburner M, Foulger R, et al. The Gene Ontology (GO) database and informatics resource. *Nucleic Acids Res* 2004;32:D258–61.
- [42] Gao H, Zhang Y, Yang L, Liu X, Guo Z, Tan Y, et al. Regulatory effects of cAMP receptor protein (CRP) on porin genes and its own gene in *Yersinia pestis*. *BMC Microbiol* 2011;11:40.
- [43] Zhang Y, Qiu Y, Gao H, Sun J, Li X, Zhang M, et al. OpaR controls the metabolism of c-di-GMP in *Vibrio parahaemolyticus*. *Front Microbiol* 2021;12:676436.
- [44] Zhang M, Cai L, Luo X, Li X, Zhang T, Wu F, et al. Effect of sublethal dose of chloramphenicol on biofilm formation and virulence in *Vibrio parahaemolyticus*. *Front Microbiol* 2023;14:1275441.
- [45] Zhang M, Luo X, Li X, Zhang T, Wu F, Li M, et al. L-arabinose affects the growth, biofilm formation, motility, c-di-GMP metabolism, and global gene expression of *Vibrio parahaemolyticus*. *J Bacteriol* 2023;205:e0010023.
- [46] Zhang M, Xue X, Li X, Wu Q, Zhang T, Yang W, et al. QsvR and OpaR coordinately repress biofilm formation by *Vibrio parahaemolyticus*. *Front Microbiol* 2023;14:1079653.
- [47] Zhang Y, Zhang T, Qiu Y, Zhang M, Lu X, Yang W, et al. Transcriptomic profiles of *Vibrio parahaemolyticus* during biofilm formation. *Curr Microbiol* 2023;80:371.
- [48] Gao H, Ma L, Qin Q, Qiu Y, Zhang J, Li J, et al. Fur represses *Vibrio cholerae* biofilm formation via direct regulation of vieSAB, cdgD, vpsU, and vpsA-K transcription. *Front Microbiol* 2020;11:587159.
- [49] Lu R, Tang H, Qiu Y, Yang W, Yang H, Zhou D, et al. Quorum sensing regulates the transcription of lateral flagellar genes in *Vibrio parahaemolyticus*. *Future Microbiol* 2019;14:1043–53.
- [50] Lu R, Sun J, Qiu Y, Zhang M, Xue X, Li X, et al. The quorum sensing regulator OpaR is a repressor of polar flagellum genes in *Vibrio parahaemolyticus*. *J Microbiol* 2021;59:651–7.
- [51] Zhang Y, Hu L, Osei-Adjei G, Zhang Y, Yang W, Yin Z, et al. Autoregulation of ToxR and its regulatory actions on major virulence gene loci in *Vibrio parahaemolyticus*. *Front Cell Infect Microbiol* 2018;8:291.
- [52] Zhang Y, Zhang Y, Gao H, Zhang L, Yin Z, Huang X, et al. *Vibrio parahaemolyticus* CalR down regulates the thermostable direct hemolysin (TDH) gene transcription and thereby inhibits hemolytic activity. *Gene* 2017;613:39–44.
- [53] Visick KL, O'Shea TM, Klein AH, Geszvain K, Wolfe AJ. The sugar phosphotransferase system of *Vibrio fischeri* inhibits both motility and bioluminescence. *J Bacteriol* 2007;189:2571–4.
- [54] Chen L, Qiu Y, Tang H, Hu LF, Yang WH, Zhu JX, et al. ToxR is required for biofilm formation and motility of *Vibrio parahaemolyticus*. *Biomed Environ Sci* 2018;31:848–50.
- [55] Gode-Potratz CJ, Kustusch RJ, Breheny PJ, Weiss DS, McCarter LL. Surface sensing in *Vibrio parahaemolyticus* triggers a programme of gene expression that promotes colonization and virulence. *Mol Microbiol* 2011;79:240–63.
- [56] Wang Y, Zhang Y, Yin Z, Wang J, Zhu Y, Peng H, et al. H-NS represses transcription of the flagellin gene *lafA* of lateral flagella in *Vibrio parahaemolyticus*. *Can J Microbiol* 2018;64:69–74.
- [57] Gode-Potratz CJ, Chodur DM, McCarter LL. Calcium and iron regulate swarming and type III secretion in *Vibrio parahaemolyticus*. *J Bacteriol* 2010;192:6025–38.
- [58] Song B, Leff LG. Influence of magnesium ions on biofilm formation by *Pseudomonas fluorescens*. *Microbiol Res* 2006;161:355–61.

- [59] Mangwani N, Shukla SK, Rao TS, Das S. Calcium-mediated modulation of *Pseudomonas mendocina* NR802 biofilm influences the phenanthrene degradation. *Colloids Surf B Biointerfaces* 2014;114:301–9.
- [60] Chalke S, Vidovic S, Fletcher GC, Palmer J, Flint S. Differential effects of magnesium, calcium, and sodium on *Listeria monocytogenes* biofilm formation. *Biofouling* 2022;38:786–95.
- [61] Oknin H, Steinberg D, Shemesh M. Magnesium ions mitigate biofilm formation of *Bacillus* species via downregulation of matrix genes expression. *Front Microbiol* 2015;6:907.
- [62] He X, Wang J, Abdoli L, Li H. Mg(2+)/Ca(2+) promotes the adhesion of marine bacteria and algae and enhances following biofilm formation in artificial seawater. *Colloids Surf B Biointerfaces* 2016;146:289–95.
- [63] Tang D, Gao Q, Zhao Y, Li Y, Chen P, Zhou J, et al. Mg²⁺ reduces biofilm quantity in *Acidithiobacillus ferrooxidans* through inhibiting Type IV pili formation. *FEMS Microbiol Lett* 2018;365.
- [64] Mulcahy H, Lewenza S. Magnesium limitation is an environmental trigger of the *Pseudomonas aeruginosa* biofilm lifestyle. *PLoS One* 2011;6:e23307.
- [65] Gotoh K, Kodama T, Hiyoshi H, Izutsu K, Park KS, Dryselius R, et al. Bile acid-induced virulence gene expression of *Vibrio parahaemolyticus* reveals a novel therapeutic potential for bile acid sequestrants. *PLoS One* 2010;5:e13365.
- [66] Kodama T, Gotoh K, Hiyoshi H, Morita M, Izutsu K, Akeda Y, et al. Two regulators of *Vibrio parahaemolyticus* play important roles in enterotoxicity by controlling the expression of genes in the Vp-PAI region. *PLoS One* 2010;5:e8678.
- [67] Kinch LN, Cong Q, Jaishankar J, Orth K. Co-component signal transduction systems: fast-evolving virulence regulation cassettes discovered in enteric bacteria. *Proc Natl Acad Sci U S A* 2022;119:e2203176119.
- [68] Wasilko NP, Larios-Valencia J, Steingard CH, Nunez BM, Verma SC, Miyashiro T. Sulfur availability for *Vibrio fischeri* growth during symbiosis establishment depends on biogeography within the squid light organ. *Mol Microbiol* 2019;111:621–36.
- [69] Yang L, Zhan L, Han H, Gao H, Guo Z, Qin C, et al. The low-salt stimulon in *Vibrio parahaemolyticus*. *Int J Food Microbiol* 2010;137:49–54.
- [70] Ball AS, Chaparian RR, van Kessel JC. Quorum sensing gene regulation by LuxR/HapR master regulators in vibrios. *J Bacteriol* 2017;199.
- [71] Zhang Y, Hu L, Qiu Y, Osei-Adjei G, Tang H, Zhang Y, et al. QsvR integrates into quorum sensing circuit to control *Vibrio parahaemolyticus* virulence. *Environ Microbiol* 2019;21:1054–67.
- [72] Chung CH, Fen SY, Yu SC, Wong HC. Influence of oxyR on growth, biofilm formation, and mobility of *Vibrio parahaemolyticus*. *Appl Environ Microbiol* 2016;82:788–96.
- [73] Wong HC, Liao R, Hsu P, Tang CT. Molecular response of *Vibrio parahaemolyticus* to the sanitizer peracetic acid. *Int J Food Microbiol* 2018;286:139–47.
- [74] Gu D, Wang K, Lu T, Li L, Jiao X. *Vibrio parahaemolyticus* CadC regulates acid tolerance response to enhance bacterial motility and cytotoxicity. *J Fish Dis* 2021;44:1155–68.
- [75] Liu B, Gao Q, Zhang X, Chen H, Zhang Y, Sun Y, et al. CsrA regulates swarming motility and carbohydrate and amino acid metabolism in *Vibrio alginolyticus*. *Microorganisms* 2021;9.
- [76] Butz HA, Mey AR, Ciosek AL, Crofts AA, Davies BW, Payne SM. Regulatory effects of CsrA in *Vibrio cholerae*. *mBio* 2021;12.
- [77] Lim JG, Choi SH. IscR is a global regulator essential for pathogenesis of *Vibrio vulnificus* and induced by host cells. *Infect Immun* 2014;82:569–78.
- [78] Lim JG, Park JH, Choi SH. Low cell density regulator AphA upregulates the expression of *Vibrio vulnificus* iscR gene encoding the Fe-S cluster regulator IscR. *J Microbiol* 2014;52:413–21.
- [79] Choi G, Jang KK, Lim JG, Lee ZW, Im H, Choi SH. The transcriptional regulator IscR integrates host-derived nitrosative stress and iron starvation in activation of the vvhBA operon in *Vibrio vulnificus*. *J Biol Chem* 2020;295:5350–61.
- [80] Houillier P, Lievre L, Hureauux M, Prot-Bertoye C. Mechanisms of paracellular transport of magnesium in intestinal and renal epithelia. *Ann N Y Acad Sci* 2023;1521:14–31.